



Spectroscopic analysis of high protein nigella seeds (Kalonji) using laser-induced breakdown spectroscopy and inductively coupled plasma/optical emission spectroscopy

Imran Rehan¹ · M. Zubair Khan¹ · Irfan Ali² · Kamran Rehan^{1,3,4} · Sabiha Sultana⁵ · Sher Shah¹

Received: 10 July 2017 / Accepted: 13 February 2018 / Published online: 20 February 2018
© Springer-Verlag GmbH Germany, part of Springer Nature 2018

Abstract

The spectroscopic analysis of high protein nigella seeds (also called Kalonji) was performed using pulsed nanosecond laser-induced breakdown spectroscopy (LIBS) at 532 nm. The emission spectrum of Kalonji recorded with an LIBS spectrometer exposed the presence of various elements like Al, B, Ba, Ca, Cr, K, P, Mg, Mn, Na, Ni, S, Si, Cu, Fe, Ti, Sn, Sr, and Zn. The plasma parameters (electron temperature and electron density) were estimated using Ca–I spectral lines and their behavior were studied against laser irradiance. The electron temperature and electron density was observed to show an increasing trend in the range of 5802–7849 K, and $(1.2\text{--}3.9) \times 10^{17} \text{ cm}^{-3}$, respectively, in the studied irradiance range of $(1.2\text{--}12.6) \times 10^9 \text{ W/cm}^2$. Furthermore, the effect of varying laser energy on the integrated signal intensities was also studied. The quantitative analysis of the detected elements was performed via the calibration curves drawn for all the observed elements through typical samples made in the known concentration in the Kalonji matrix, and by setting the concentration of P as the calibration. The validity of our LIBS findings was verified via comparison of the results with the concentration of every element find in Kalonji using the standard analytical tool like ICP/OES. The results acquired using LIBS and ICP/OES were found in fine harmony. Moreover, limit of detection was measured for toxic metals only.

1 Introduction

Nigella sativa also called as “Kalonji” in local languages is a good source of nutritional as well as essential elements [1–3]. It is also known as black cumin seeds are widely used in Pakistan and Middle Eastern countries as a spice in cuisines, due to its pungent and bitter taste. Literature survey reports that the nigella seeds have many medicinal

properties. These are used for treatment of asthma, digestion disorder, as well as carminative, aromatic, diuretic, stomachic, and diaphoretic problems [4–6]. That is why it is often known as the cure of all diseases. This seeds have found to have higher concentration of potassium ‘K’ as compared to camel milk [7]. The enhanced health potential of Kalonji has been attributed to its active ingredients [8]. The conventional techniques applied for elemental study of Kalonji are inductively coupled plasma optical/emission spectroscopy (ICP/OES), inductively coupled plasma/mass spectroscopy (ICP/MS), neutron activation analysis (NAA) and gas liquid chromatography (GLC), and proton induced X-ray emission (PIXE) spectroscopy [9–12], but these methods require lengthy sample preparation and boring pretreatment procedures, process of acid digestion at high temperature and pressure, as well as the use and clearance of dangerous chemicals which are harmful to our environment. Laser-Induced Breakdown Spectroscopy (LIBS) is a versatile methodology able to analyze the sample in its original form and thereby catching up from their point of limitations of other methods in terms of extended sample preparation that might lead to the change of chemical composition of the original sample. This method has much application in the

✉ Imran Rehan
irehanyousafzai@gmail.com

¹ Department of Applied Physics, Federal Urdu University of Arts, Science and Technology, Islamabad 44000, Pakistan

² Department of Physics, University of Engineering and Technology, Lahore 54890, Pakistan

³ State Key Laboratory of Magnetic Resonance and Atomic & Molecular Physics, Wuhan Institute of Physics and Mathematics, UCAS, Wuhan 430071, People’s Republic of China

⁴ School of Physics, University of Chinese Academy of Sciences, Beijing, People’s Republic of China

⁵ Department of Chemistry, Islamia College University, Peshawar 25120, Pakistan

qualitative and quantitative elemental analysis of materials [13–18].

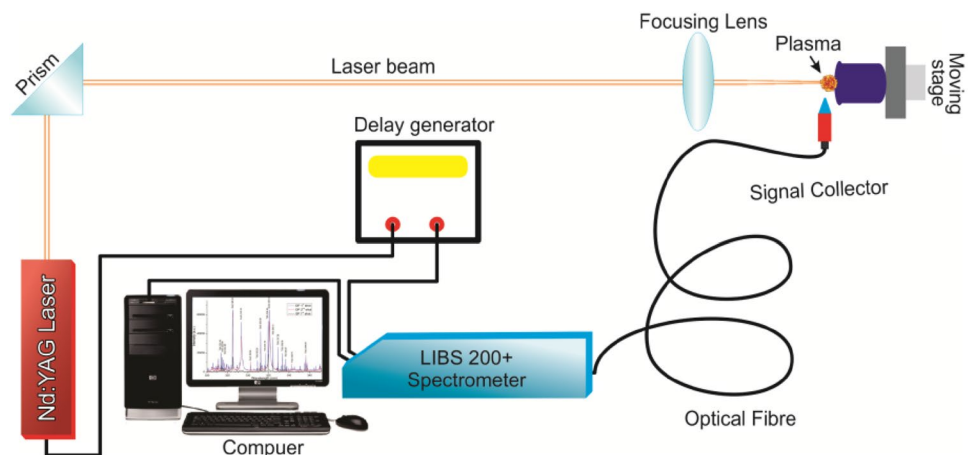
The present work was performed to use LIBS to study the elemental composition and percentage abundance of elements present in Kalonji in Pakistan. The Kalonji is used commonly due to different good health properties. The Kalonji sample was collected from a local market, and dried and crushed into a fine powder to make the pellets that were placed to laser light to record the emission spectra. The percentage concentrations of the detected elements in the sample were estimated by calibration curves method, the slope of these curves was utilized for estimation of the sensitivity of our LIBS system in accordance with the definition of International Union of Pure and Applied Chemistry (IUPAC) and by setting the concentration of most abundant element as the calibration. The results of LIBS were compared to analyses performed via ICP spectroscopy which were in excellent agreement. The outcomes of ICP/OES were more precise, but this approach requires more time and sample preparation, while LIBS is easy and the results can be obtained with very sample preparation.

2 Experimental

The experimental sketch is exposed in Fig. 1. Briefly, it is composed of a laser, a motorized translational sample's stand, a high-resolution spectrometer (LIBS2000+, Ocean Optics, USA), a charged coupled device (CCD), and a personal computer for controlling and acquisition of data. A Nd:YAG laser (Quantel Brilliant, France) with a maximum pulse energy of 200 mJ/pulse at the second harmonic wavelength of 532 nm, pulsed duration of 5 ns, and a maximum repetition rate of 10 Hz (Pulse/sec) was used as energy source. The laser has the potential of delivering a maximum energy of 400 mJ/pulse at fundamental mode (1064 nm) and 200 mJ/pulse at second harmonic (532 nm). The Nd:YAG

pulsed laser oscillator uses laser polarizer. The characteristic of polarizer is such that it does not transmit until beam or light is only horizontally polarized. Hence, the polarizer causes the light transmission and we get minimal losses with Gaussian beam profile. The laser was focused on to the surface of the sample at ambient pressure using a convex lens of 30-cm focal length. The focusing lens was mounted onto the translation stage to adjust the distance of lens-to-sample. The optical emissions from the laser-produced plasma were acquired through a 5-cm diameter fused silica window connected with 2-m fiber optic cable (high-OH, core diameter: 600 μm) having a collimating lens (0° – 45° field of view) placed at right angle to the direction of the plasma expansion and transferred to a high-resolution multichannel spectrometer LIBS 2000-plus for dispersion and detection. The LIBS2000 system was equipped with five high-resolution miniature fiber optic spectrometers, each having a slit width of 5 μm and a 2048-element linear CCD array that provides an optical resolution of ≈ 0.06 nm (Full width at half maximum). Each spectrometer has different numbers of grooves density on the grating (2400 and 1800 lines/mm), in such a way that high resolution (HR1) has groove density of 2400 (lines/mm) with bandwidth of ~ 200 – 300 nm in UV region, HR2 has groove density of 2400 (lines/mm) with bandwidth of ~ 300 – 400 nm in UV region, HR3 has groove density of 1800 (lines/mm) with bandwidth of ~ 400 – 500 nm in visible region, HR4 has groove density of 1800 (lines/mm) with bandwidth of ~ 500 – 600 nm in visible region, and HR5 has groove density of 1800 (lines/mm) with bandwidth of ~ 600 – 720 nm in visible region. To collect the optical spectra, the detector and the Q-switch of the Nd:YAG laser were synchronized. The flash lamp out of the Nd:YAG laser triggered the detector through a four-channel digital delay generator (SRS DG, 535). The LIBS2000+ detector triggered the Q-switch of the Nd:YAG laser. A delay time of 1.0 ms and an integration time of 0.4 μs were selected. The output data acquired concurrently via all the five spectrometers

Fig. 1 Schematic diagram of LIBS experiment setup



were stored in a personal computer via the OOILIBS application software for further analysis.

To reduce pulse-to-pulse variation in LIBS signal intensity, we used online measurement of pulse energy. During the experiment, we have used 10% beam splitter and the laser energy was monitored for each laser shot. In this way, we only used data of laser shots having minimum pulse-to-pulse intensity variation. Each of the spectra was obtained by averaging 30 laser shots under the same experimental conditions, to improve the LIBS sensitivity and selectivity by minimizing the statistical error owing to laser shot-to-shot variations. A calibrated energy meter (Coherent, Field Max II) was engaged to measure the laser energy. The detection limit for toxic elements under investigation was also calculated. Limit of detection (LOD) here means the lower abundance that can be detected by LIBS. The LOD was predicted using Eq. [19]:

$$\text{LOD} = \frac{2\sigma}{S}, \quad (1)$$

where σ stands for the standard deviation of the background (noise level); S stands for calibration sensitivity (S = slope of the calibration curve) which is the ratio of the line intensity versus concentration. To diminish the unintended measurement errors, the spectrometer was turned on, and first, all types of electronic noise (e.g., CCD dark current) were recorded by spectrometer with long enough delay time and laser pulse of lower energy independently and were subtracted from the measured spectra earlier before saving using system built-in facility (OOILIBS2000 software).

2.1 Preparation of sample for LIBS analysis

In this study, the Kalonji sample was procured from the local market located in Rawalpindi city of Pakistan. To make pellets from the sample, the sample was first placed in a desiccator to complete dry. The complete dried sample was then crushed to fine powder and was then placed in a cylindrical dye (2-cm diameter and 2-mm thickness) and then pressed hard using hydraulic press into circularly shaped pellets that was fitted in the LIBS system sample holder. The pellets were quite hard enough to withstand the thrust of laser pulse without adding any binder.

2.2 Preparation of sample for ICP analysis

For the analysis of Kalonji sample using ICP/OES technique, 0.05 g of the Kalonji sample was weighed with an analytical balance, added 5 ml of nitric acid (99%, Fisher Scientific), then heated at ~ 60 °C for appropriate dissolution of metals in acid. The solution was waited to cool down then added 35 ml of DI water to the resultant solution and further heated at 40 °C for 2 h for the complete digestion of the

Kalonji sample. The solution was waited to cool down and the un-dissolved particles were removed using filter paper. The filtrate form of sample was studied using Optima 2100 DV ICP/OES (optical emission system). Optima 2100 DV system has high-dispersion Echelle spectrometer with a focal length of 0.3 m. The Echelle grating used for dispersion has 79 lines/mm with a blaze angle of 63.40 covering the spectral range from 160 to 900 nm with resolution of < 0.009 @ 200 nm. The system included complete dual-viewing optics under computer and software control. The instrumental functions including plasma ignition, flow of gas, viewing position, and monitoring of safety interlocks were fully controlled using WinLab32 software. The Optima 2100 DV detection system has UV-sensitive, dual backside-illuminated CCD array detector having two photosensitive segments containing 176 by 128 pixels. Earlier to perform quantitative analysis, first selected the elements to be analyzed.

The various conditions used in the ICP analysis are tabulated as below in Table 1.

3 Results and discussion

In the first step, prior to performing experiments on actual sample, the distance of lens-to-sample was optimized for the Nd:YAG laser. The distance of lens-to-sample has strong influences on the ablated mass, plasma temperature, and on the repeatability of the optical spectra [20, 22]. Therefore, we optimized the distance of lens-to-sample by investigating the effect of its separation on the quality of spectra. In our case, it was optimized to be ~ 29 cm. In the second step, we recorded the emission spectra from the laser-produced Kalonji plasma and studied to classify all the observed transitions, as shown in Fig. 2.

The emission spectrum was recorded at a distance of 0.25 mm from the target surface using the Nd:YAG pulsed laser ($\lambda = 532$ nm) at an average for 30 laser shots. The presence of hydrogen line was owing to water in the surrounding air. We further confirmed our analysis by comparing the LIBS

Table 1 Instrumental parameters used for ICP/OES

| Detector | Solid-state detector |
|-----------------------------|----------------------|
| Operating power (W) | 1300 |
| Sample flow rate (mL/min) | 1.500 |
| Nebulizer gas flow (L/min) | 0.800 |
| Plasma gas flow (L/min) | 15.00 |
| Supporting gas flow (L/min) | 0.200 |

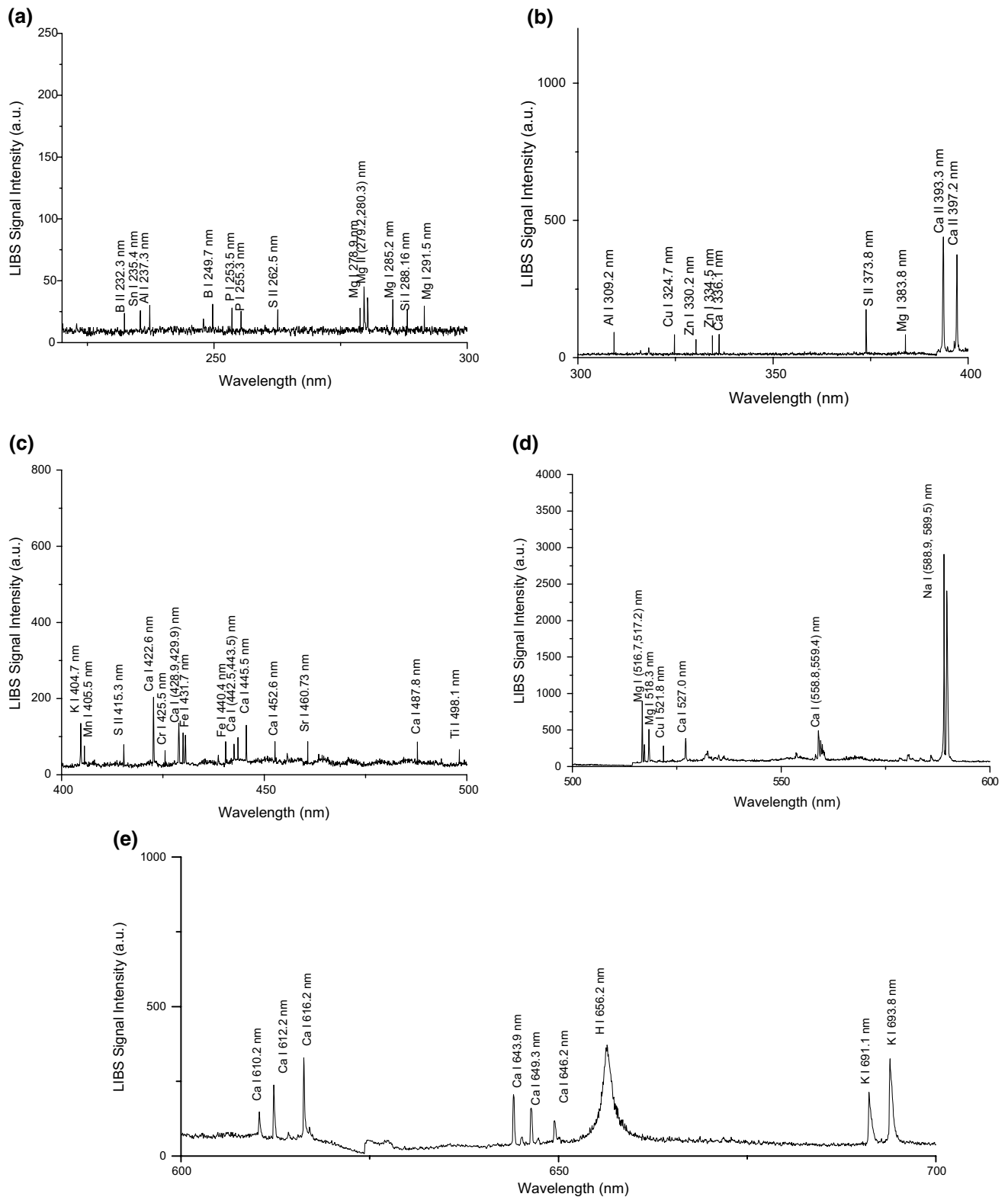


Fig. 2 Emission spectrum of Kalonji using pulsed Nd:YAG laser @ 532 nm

spectra of Kalonji with individual LIBS spectra of the pure elements.

The careful investigation of emission spectrum consists of the neutral and singly ionized lines of boron, sulfur, calcium, magnesium, and titanium, along with the neutral lines aluminum, phosphorous, silicon, zinc, manganese, copper, potassium, sodium, and chromium. All the transitions in spectra were identified using the handbook of basic atomic spectroscopy data [19].

For the quantitative estimation of detected elements in Kalonji sample, the selected atomic lines were, Cr-I 425.5 nm, Cu-I 521.83 nm, Mn-I 405.5 nm, Ni-I 335.1 nm, P-I 255.5 nm, Fe-I 440.4 nm, Al-I 309.2 nm, B-I 249.7 nm, Ba-I 553.5 nm, Ca-I 649.3 nm, Mg-I 518.3 nm, K-I 404.7 nm, Na-I 588.9 nm, S-II 373.8 nm, Si-I 288.16 nm, Sr at 460.73 nm, Sn at 235.4 nm, Ti at 498.1 nm, and Zn at 330.2. The reason for selecting those particular atomic transition lines was because they were intense, isolated, and well-resolved atomic transition lines in the spectral region.

3.1 Parameters of laser-induced plasma (electron temperature and number density)

To do a quantitative and the qualitative analysis of target under test and to analyze the properties of plasma parameters, the study of emission generated from laser-induced plasma (LIP) is very imperative. Plasma temperature (T_e), electron density (N_e), and the number density of the emitting elements are the basic properties of plasma. The determination of plasma parameters is very essential to justify the condition that plasma is optically thin and the Local Thermo dynamic Equilibrium which are significant for the LIBS quantitative investigation. In case the plasma does not satisfy the Thermo dynamic Equilibrium state, as a result, there may be strong self-absorption which results in an in-accurate measurement of the quantitative analysis. Furthermore, the knowledge of LIP temperature is imperative to understand the processes such as atomization, dissociation, and excitation as well as for the improvement of LIBS Sensitivity. The T_e was estimated with the Boltzmann plot method described by the relation [15, 20–22]:

$$\ln\left(\frac{I_{ij}\lambda_{ij}}{A_{ji}g_i}\right) = \ln\left(\frac{N(T)}{U(T)}\right) - \frac{E_i}{kT_e}, \quad (2)$$

where λ_{ij} is the wavelength of transition, A_{ji} is called the transition probability, g_i gives the statistical weight of the upper energy level E_i , k is the Boltzmann constant, and T_e is the electron temperature. The value of $\ln\left(\frac{I_{ij}\lambda_{ij}}{A_{ji}g_i}\right)$ for each transition can be plotted as a function of upper state energy E_i and fitted with a straight line, the temperature T_e is given by the slope $\left(-\frac{1}{kT_e}\right)$ of straight line. In this work, T_e was

estimated using five transitions of neutral calcium at 336.1, 443.5, 3445.5, 643.9, and 452.6 nm, for which the needed spectroscopic parameters were taken from NIST database.

A representative Boltzmann plot of the neutral calcium lines is exposed in Fig. 3. The electron temperature determined from the slope of the straight line was 7849 K. The electron temperature determined was similar within $\pm 10\%$, this uncertainty temperature mainly comes due to uncertainties in the transitions probabilities and measuring the integrated intensity of the emission lines.

The N_e was measured from the Stark-broadened line profile of the neutral calcium transition ($3p^64s4p\ ^1P_1^0 \rightarrow 3p^64s^2\ ^1S^0$) at 422.67 nm. In LI plasmas, the dominant broadening mechanism is Stark broadening. For the purpose to get the correct value of the N_e , the line profile was corrected by subtracting the contributions from the Doppler (0.005 nm determined at 7849 K) and instrumental broadening (0.05-nm). The uncertainty in the estimated value of electron density was 10%, which was generally due to the uncertainty in the determination of the electron impact parameter (ω) and in measurement of full width at half maximum of Lorentzian line profile. The major contribution of Stark broadening comes from electrons as they have higher relative velocities, although both ions and electrons are responsible for the contribution. The full width at half maximum (FWHM) of a Stark-broadened line $\Delta\lambda_{FWHM}$ is related to N_e ($/\text{cm}^3$) through the following relation:

$$N_e = \frac{\Delta\lambda_{FWHM}}{2w} \times 10^{16}. \quad (3)$$

The Stark-broadened line profile is \sim Lorentzian, so the spectral emission line was fitted using Lorentzian function to estimate the FWHM, whereas the stark broadening parameter 'w' was taken from [23].

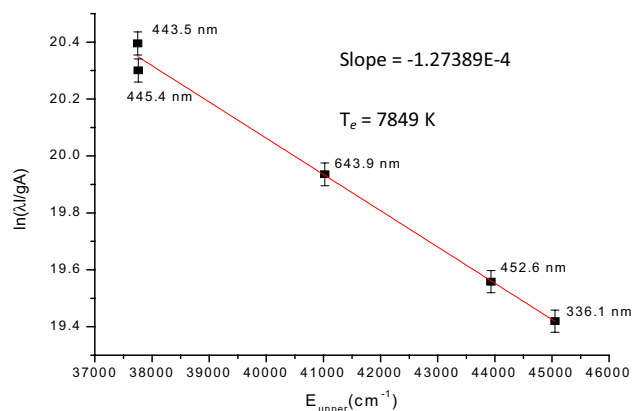


Fig. 3 Typical Boltzmann plot for the determination of the electron temperature using six neutral calcium emission lines

One of the assumptions that guarantee the condition of optically thin plasma is criterion known as the McWhirter criterion which can be formulated as follows:

$$N_e(\text{cm}^{-3}) \geq 1.6 \times 10^{12} T_e^{\frac{1}{2}} (\Delta E)^3, \tag{4}$$

where ΔE is the energy difference of oscillations responsible for spectral emission associated.

The measured value of N_e was $3.9 \times 10^{17} \text{ cm}^{-3}$. The plasma temperature (maximum) determined by the Boltzmann plot technique was $7849 \pm 250 \text{ K}$. This value of temperature used in the mathematical formula for McWhirter's criterion along with value of difference of energy between the associated energy levels of respected transition of calcium neutral emission line at wavelength 422.67 nm furnishes the electron number density of about $3.5 \times 10^{15} \text{ cm}^{-3}$ that was less than the value determined experimentally and hence shows the agreement of the McWhirter's criterion. This indicates that plasma was near to thermo dynamic equilibrium (LTE). Similarly, all the measured values were verified using Eq. (4). To give further information, we determined the electron number density using Mg-I at 285.21 nm as $3.5 \times 10^{17} / \text{cm}^3$ and got verified using Eq. (4). In a similar way, electron temperatures was also approximated utilizing Mg lines (at 278.29, 291.54, 383.82, and 389.19 nm) and were found similar within $\pm 10\%$ uncertainty with the temperature measured using Ca lines.

The laser generated plasma via an intense laser beam is believed to be optically thin if the ratio of the intensity of two interference-free emissions from a species of same higher level has a similar value as their the corresponding ratio between the associated transition probabilities under the experimental uncertainty [24, 25]. For this purpose, the ratios of neutral emission lines from calcium and magnesium were compared with the ratios of the associated transition probabilities taken from the NIST database. The ratio of

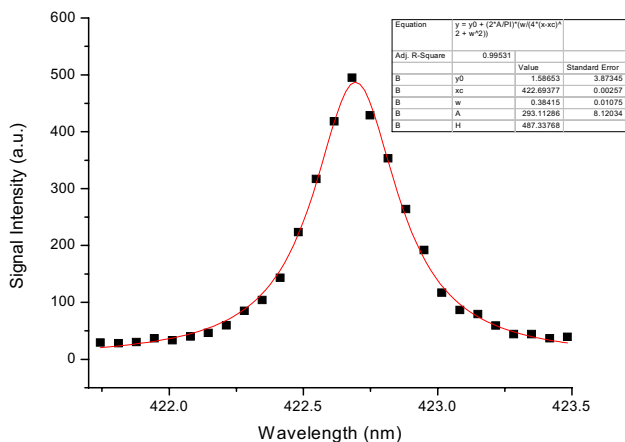


Fig. 4 Stark-broadened line profile of neutral Ca transition at 422.67 nm corresponding to $(3p^6 4s 4p \ ^1P^0_1 \rightarrow 3p^6 4s^2 \ ^1S^0_0)$ transition

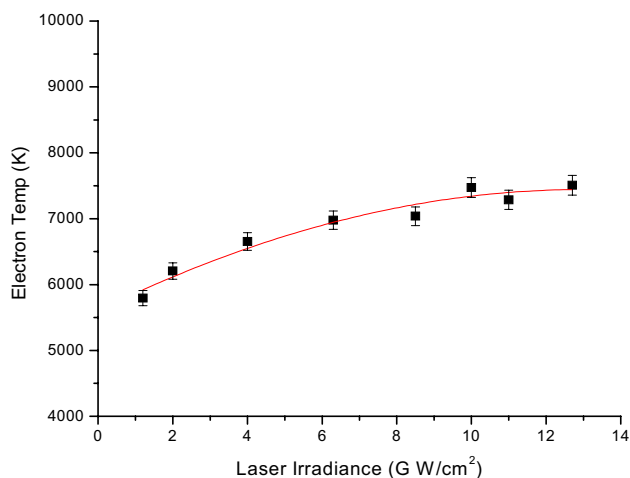


Fig. 5 Plot showing variation in electron temperature with laser irradiance. The solid line shows the power-law fitting

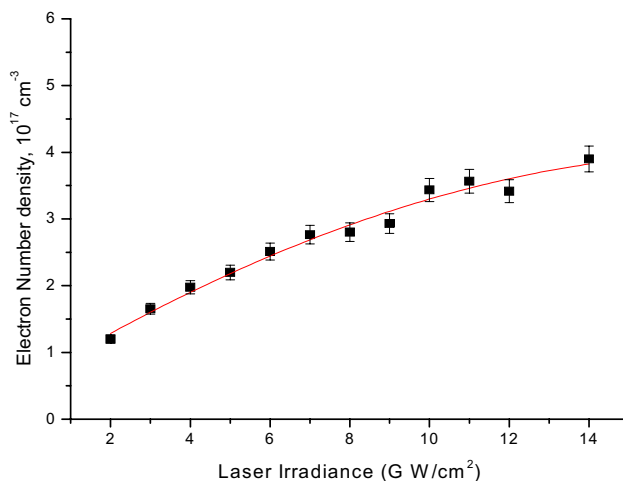


Fig. 6 Plot showing the variation in electron number density with laser irradiance. The solid line shows the power-law fitting of the experimental data points

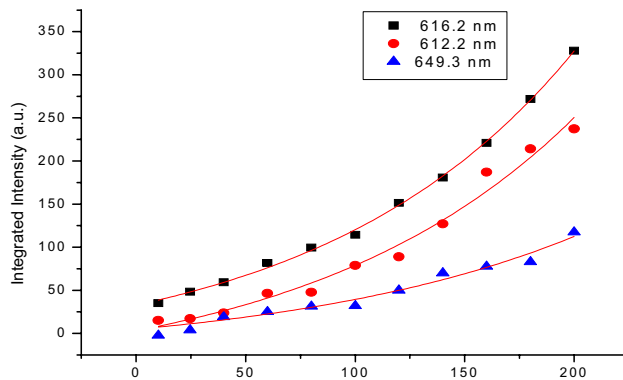
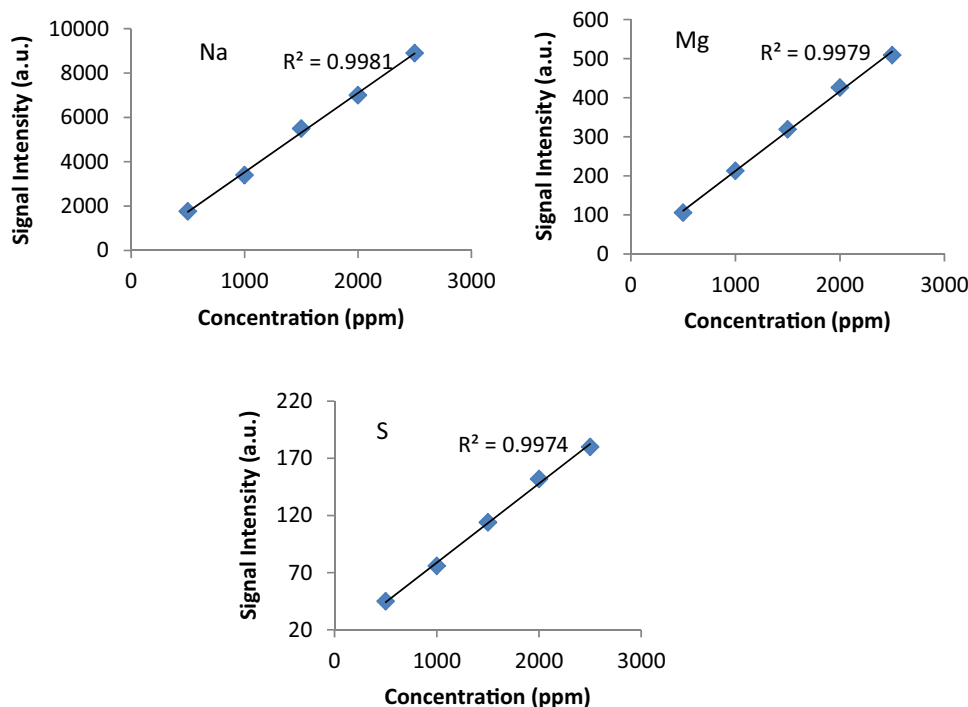


Fig. 7 Variation in spectral line intensities of neutral calcium (616.2, 612.2, and 643.9 nm) with laser energy

Fig. 8 Calibration curves for Na, Mg, and S respectively



Ca-I at 428.94 nm/at 429.90 nm was found as 1.23, whereas the ratio of their transition probabilities was 1.29. In a similar way, the ratio of Mg-I at 516.73 nm/at 517.27 nm was 2.91, whereas the ratio of their related transition probabilities was 2.97. Such consistency among the ratios of intensity and their transition probabilities exhibit obviously that plasma generated is thin optically.

The effects of laser irradiance on the electron temperatures were also studied. The temperature was found to vary from 5802 to 7849 K with an increase in laser irradiance from $(1.20 \text{ to } 12.7) \times 10^9 \text{ W/cm}^2$. In a similar way, the N_e was found to increase from 1.2×10^{17} to $3.9 \times 10^{17}/\text{cm}^3$ for the same laser irradiance.

The observed increase in plasma parameters (T_e and N_e) with the corresponding enhancement in laser irradiance was owing to the fact that, at higher laser irradiance, the formation of plasma and absorption of laser radiation takes place concurrently.

At the elevated values of laser irradiance, more excited species (ionic and neutral) are generated. Further heating and ionization take place as a result of the interaction of laser pulse with these species. As a consequence, the consumption of in-coming laser energy increases. The steady variation/saturation of T_e and N_e at higher values of laser irradiance is attributed to the plasma shielding effect, i.e., b/c of the reflection or absorption of laser energy with the plasma. Since the present experiment was performed at ambient pressure, the plasma shielding effect due to air confines the ionization by decreasing the efficiency of the laser irradiance present for the mass ablation.

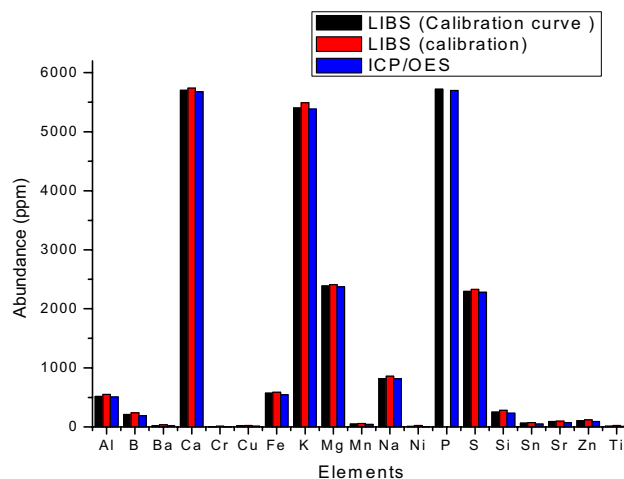


Fig. 9 Graph showing comparison of the concentrations of detected elements in Kalonji using two LIBS calibration procedures and ICP/OES

Figure above depicts the changes in signal intensities of Ca-I emission lines, the signals increase as the laser pulsed energy increases (Figs. 4, 5, 6, 7).

3.2 Quantitative study of Kalonji sample

For the quantitative analysis of Kalonji, we applied two LIBS approaches: the calibration curve technique and by setting the concentration of P as the calibration.

In the first method, the calibration curves were constructed based on various set of samples (generally more than three) with various known concentration of a particular analyte. The calibration curves provide a way to approximate the abundance of a particular species in an unknown sample. The plot of emission line intensities of the particular elements against its abundance yields the calibration curve. Figure 8 shows the typical calibration curves (Mg, Na, and S) in the Kalonji sample. Each value of R^2 (see Fig. 8) indicates the precision of our linear-fit (i.e., R-squared is nearly equal to 1).

In the second method, the concentration of detected elements in the test sample was approximated by measuring the integrated intensities of spectral emission lines, then the concentration of observed elements was measured by setting the concentration of most abundant element as the calibrate.

As phosphorous was the most abundant among all of the detected elements in the test sample; therefore, 'P' was taken as the calibration.

At last, the relative abundance was determined by dividing the concentration of particular element to the total concentration of all the observed elements.

For confirmation of our LIBS quantitative results, we estimated the abundance of all the species in the Kalonji sample by means of standard analytical tool like ICP/OES. Both the results were in excellent agreement, as depicted in Fig. 9.

The essentials like Ca (5700) ppm, K (5400) ppm, P (5718) ppm, Mg (2389) ppm, and S (2298) were found to be most abundant in the test sample. The concentration of toxic elements like Cr, Cu, and Ni was 8, 22, and 10 ppm respectively. The trace elements Ba, and Ti were 19 and 15, respectively. Other metals like B, Na, Mn, Si, Sn, and Sr were of the amount of 210, 822, 50, 250, 62, and 90 ppm respectively.

Among the detected toxic metals, Zn (105 ppm) was found to be more abundant. The LOD estimated for Cr, Cu, Ni, and Zn were 4, 8, 3, and 30 respectively. All the measurements were made under the condition of LTE and OTP.

4 Conclusion

The spectroscopic investigation of Kalonji plasma was carried out in air to determine the composition and abundance of elements in the test sample. The elements like, Al, B, Ba, Ca, Cr, K, P, Mg, Mn, Na, Ni, S, Si, Cu, Fe, Ti, Sn, Sr, and Zn were confirmed to be present in Kalonji. The comparative analysis of LIBS with ICP/OES showed that using the calibration curves method provided the closest results to the values obtained by ICP/OES. The most abundant elements in Kalonji were Ca, P, S, K, and Mg. In addition, the plasma

temperature was estimated using the selected neutral lines of Ca via the Boltzmann plot. The electron number density was determined from Stark-broadened line profiles. The plasma was characterized in terms of T_e and N_e with respect to the laser radiance. The effect of varying laser energy on the integrated signal intensities was also studied. The T_e and N_e were found to increase with the increase of laser irradiance. The LOD was measured for detected toxic metals only.

References

1. J.D. Bewley, M. Black, P. Halmer, *The Encyclopedia of Seeds: Science, Technology And Uses* (CABI, 2006)
2. M.B. Atta, *Food Chem.* **83**, 63 (2003)
3. M.S. Butt, M.T. Sultan, *Crit. Rev. Food Sci. Nutr.* **50**, 654 (2010)
4. M.S. Al-Jassir, *Food Chem.* **45**, 239 (1992)
5. V. Babayan, D. Koottungal, G. Halaby, *J. Food Sci.* **43**, 1314 (1978)
6. R. Agarwal, M. Kharya, R. Shrivastava, *Indian J Exp Biol.* **17**, 1264 (1979)
7. A. Al-Attas, *Arab. J. Nucl. Sci. Appl.* **42**, 59 (2009)
8. M.F. Ramadan, *Int. J. Food Sci. Technol.* **42**, 1208 (2007)
9. S. Khaled, M. Mouzai, A. Ararem, L. Hamidatou, B. Zouranen, *J. Radioanal. Nucl. Chem.* **281**, 87 (2009)
10. Ş. Tokaloğlu, *Food Chem.* **134**, 2504 (2012)
11. M.A. Ali, M.A. Sayeed, M.S. Alam, M.S. Yeasmin, A.M. Khan, I.I. Muhamad, *Bull. Chem. Soc. Ethiop.* **26** (2012)
12. K.T. El Araqi, J. Gilot-Delhalle, I. Roelandts, G. Weber, R. Del-tova, J. Moutschen, *Environ. Exp. Bot.* **38**, 87 (1997)
13. L.J. Radziemski, *Spectrochim. Acta Part B* **57**, 1109 (2002)
14. V. Babushok, F. DeLucia, J. Gottfried, C. Munson, A. Miziolek, *Spectrochim. Acta Part B* **61**, 999 (2006)
15. J.P. Singh, S.N. Thakur, *Laser-Induced Breakdown Spectroscopy* (Elsevier, Amsterdam, 2007)
16. R.A. Multari, D.A. Cremers, J.A.M. Dupre, J.E. Gustafson, *J. Agric. Food Chem.* **61**, 8687 (2013)
17. I. Rehan, K. Rehan, S. Sultana, M.O. ul Haq, M.Z.K. Niazi, R. Muhammad, *Eur. Phys. J. Appl. Phys.* **73**, 10701 (2016)
18. A. Ali, M. Khan, I. Rehan, K. Rehan, R. Muhammad, *J. Spectrosc.* **2016** (2016)
19. J.E. Sansonetti, W.C. Martin, *J. Phys. Chem. Ref. Data.* **34**, 1559 (2005)
20. M. Qian, C. Ren, D. Wang, J. Zhang, G. Wei, *J. Appl. Phys.* **107**, 063303 (2010)
21. A.W. Miziolek, V. Palleschi, I. Schechter, *Laser Induced Breakdown Spectroscopy* (Cambridge University Press, Cambridge, 2006)
22. D.A. Cremers, F.Y. Yueh, J.P. Singh, H. Zhang, *Encyclopedia of Analytical Chemistry* (Wiley, Hoboken, 2006)
23. H. Griem, *Principles of Plasma Spectroscopy* (Cambridge University Press, Cambridge, 1997)
24. H.R. Griem, *Plasma Spectroscopy* (McGraw-Hill, New York, 1964)
25. L.J. Radziemski, T.R. Loree, D.A. Cremers, N.M. Hoffman, *Anal. Chem.* **55**, 1246 (1983)